

EFFECT OF FLUID DISPERSION COEFFICIENTS ON PARTICLE-TO-FLUID HEAT TRANSFER COEFFICIENTS IN PACKED BEDS

CORRELATION OF NUSSELT NUMBERS

N WAKAO,[†] S KAGUEI and T FUNAZKRI

School of Engineering, Yokohama National University, Hodgaya-ku, Yokohama, Japan 240

(Received 24 February 1978, accepted 17 May 1978)

Abstract—The published heat transfer data obtained from steady and nonsteady measurements are corrected for the axial fluid thermal dispersion coefficient values proposed by Wakao[1]

The corrected data in the range of Reynolds number from 15 to 8500 are correlated by the analogous form of the mass correlation proposed by Wakao and Funazkri[2]

$$Nu = 2 + 1.1 Pr^{1/3} Re^{0.6}$$

This work for particle-to-fluid heat transfer is an extension of that reported by Wakao and Funazkri[2] in which the published particle-to-fluid mass transfer data were corrected for axial fluid dispersion coefficients. Similarly to the data collection for mass transfer, we confine ourselves to the heat transfer measurements which satisfy the following conditions

1. Particles in bed being all active
2. Number of particle layers in heat transfer bed being greater than two

Table 1 summarizes the experimental conditions of the collected measurements. The data are shown as Nu vs Re in Fig. 1. Considerable scattering and anomalous decrease in Nusselt number are seen at low Reynolds numbers.

In fact, the anomaly of Nusselt numbers has been a subject of discussion for long. However, not all the experimental investigators have supported the anomaly of Nusselt numbers. From frequency response measurements, Littman and Shiva[3], and Gunn and De Souza[4] have estimated, respectively, from their own experiments the limiting Nusselt numbers of about 0.4 and 10.

Some theoretical studies have also been made on this subject. There is, of course, no exact theory which describes the transport phenomena in packed beds. Different theoretical estimates have given different limiting Nusselt numbers. Just like the experimental data, the two completely divergent conclusions have been drawn from the estimates.

Cornish[5] indicates, assuming an analogy between electrostatics and heat, that the heat transfer coefficient in dense system of particles is considerably smaller than that for a single sphere in an infinite medium. Kunii and Suzuki[6] point out that flow channeling in the bed is the reason for the anomaly. Nelson and Galloway[7] indicate that the anomaly is explained by a renewal of fluid

element surrounding each particle. Schlunder[8] shows, on the assumption that packed bed is a bundle of parallel capillaries, that transfer coefficients decrease with a decrease of flow rate at lower Reynolds numbers.

On the other hand, Pfeffer and Happel[9] obtain, by applying a free surface model, a limiting Nusselt number of about 13 at the bed void fraction 0.4. From an analysis of steady transfer in a stagnant fluid in a concentric hollow sphere, Miyauchi[10] shows a limiting Nusselt number of about 18 at the bed void fraction 0.4. Sørensen and Stewart[11] study a creeping flow through a cubic array of spheres to find a limiting Nusselt number of about 3.9.

Wakao *et al.* [1, 12–14], however, find the defect of the fundamental equations responsible for the anomalous decrease in Nusselt number at lower Reynolds numbers.

REVIEW AND CORRECTION OF THE DATA OBTAINED FROM STEADY MEASUREMENTS

Simultaneous heat and mass transfer study: evaporation of water and diffusion-controlled chemical reaction on particle surface

The mass transfer data obtained from the simultaneous heat and mass transfer studies have been used for the data correlation in the mass transfer paper[2]. The corresponding heat transfer data are, therefore, used in the present paper. The data are those obtained from the measurements of evaporation of water by Hougen *et al.* [15, 16], Hurt[17], Galloway *et al.* [18], Thodos *et al.* [19–23] and Bradshaw and Myers[24], and those determined from the catalytic decomposition of hydrogen peroxide on metal spheres by Satterfield and Resnick[25].

The measurements were made with solid particles having constant surface temperatures throughout the beds. In the studies the system was described as

$$U \frac{dT_F}{dx} + \frac{h_p a}{\epsilon_b C_F \rho_F} (T_F - T_p) = 0 \quad (1)$$

[†]To whom correspondence should be made.

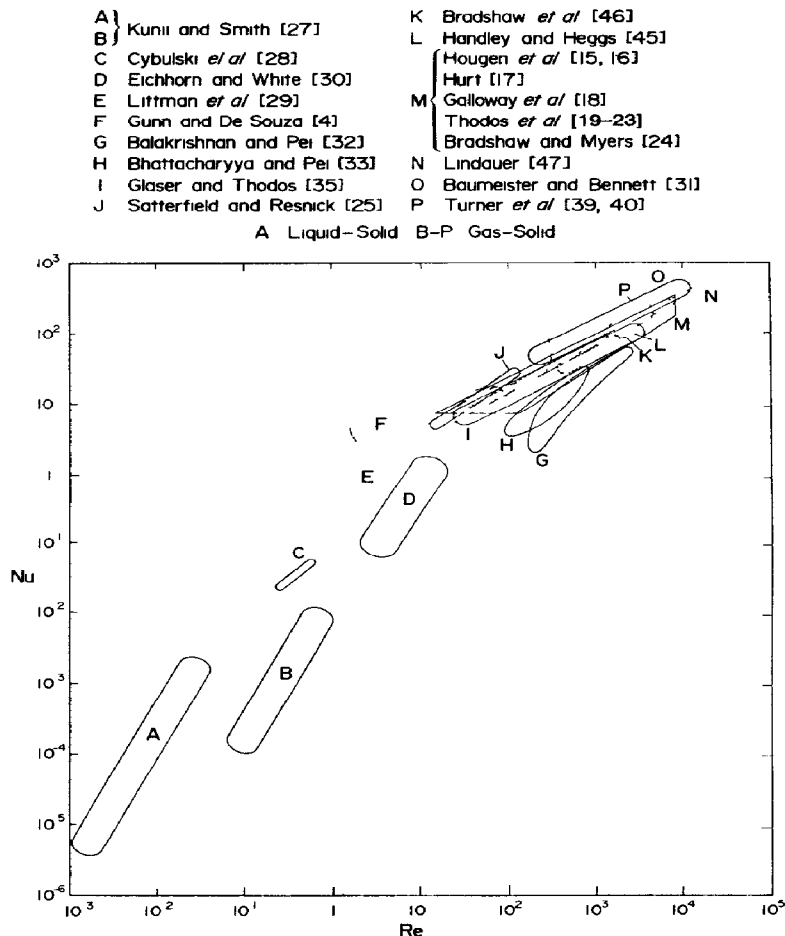


Fig 1 Heat transfer data published in the literature

and the heat transfer coefficients, h_p , have been determined

If, however, axial fluid thermal dispersion is considered, the system is

$$U \frac{dT_F}{dx} + \frac{h_p a}{\epsilon_b C_F \rho_F} (T_F - T_{ps}) = \alpha_{ax} \frac{d^2 T_F}{dx^2} \quad (2)$$

The axial fluid thermal dispersion coefficient α_{ax} has been considered as $\alpha_{ax} = (0.6 - 0.8)\alpha_F$ in laminar flow range and $\alpha_{ax} = 0.5 D_p U$ in turbulent flow range, or approximately over the range from laminar to turbulent

$$\alpha_{ax} = (0.6 - 0.8)\alpha_F + 0.5 D_p U \quad (3)$$

Wakao[1] and coworkers[12, 14], however, recently pointed out that the heat transfer coefficients should be determined from eqn (2) with the following α_{ax}^* values (as described later, this is called the modified D-C model) instead of α_{ax} of eqn (3)

$$\alpha_{ax}^* = \frac{k_{e,ax}}{\epsilon_b C_F \rho_F} \quad (4)$$

The axial fluid dispersion is expressed by eqn (3), but the right hand side of eqn (2) should have solid-phase conduction contribution, as well as the dispersion in fluid phase. Therefore, α_{ax}^* should rather be called the effective dispersion coefficient

The heat transfer measurements reviewed in this section have been made in the Reynolds number up to 8500. As far as the authors know, no measurements have been made on $k_{e,ax}$ at such high flow rates. At high flow rates, however, the axial fluid dispersion is, as described before, expressed as a Peclet number of two. Equation (4) is, therefore, rewritten as

$$\alpha_{ax}^* = \frac{k_e^0}{\epsilon_b C_F \rho_F} + 0.5 D_p U \quad (5)$$

where k_e^0 is the effective thermal conductivity of a stagnant packed bed. Note that Wakao and Kato[26] have given a chart for estimating k_e^0 values

The heat transfer coefficients are recalculated from all of the steady heat transfer studies reviewed in this section except the papers [15, 17, 24] in which no detailed data on bed height and/or void fraction are given. The

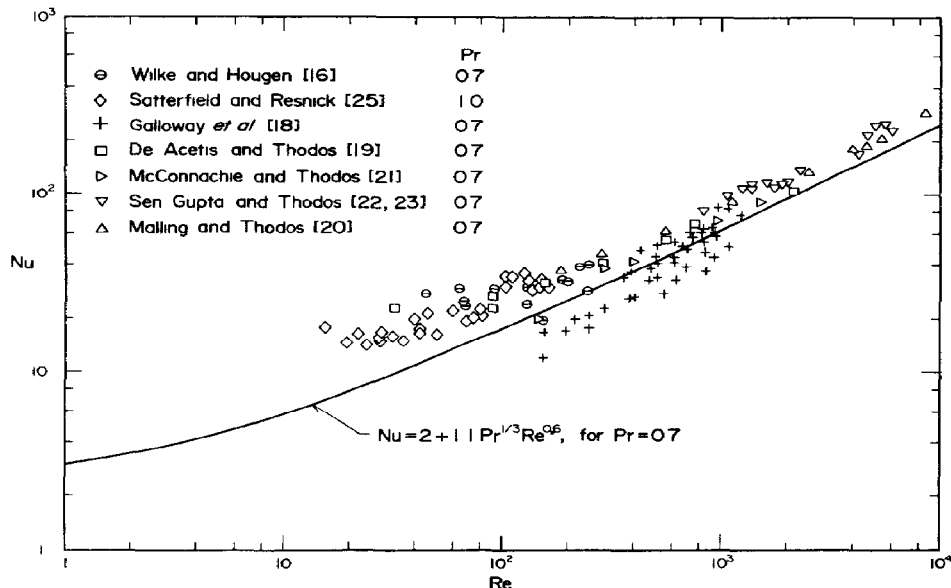


Fig. 2 Heat transfer data of steady state measurements corrected for α_{sx}^*

correction procedure is identical with that employed in the mass transfer study [2] except for the difference between heat and mass. This is briefly described in Appendix A.

The corrected data are plotted as Nu vs Re in Fig. 2. The solid line shows the analogous form of the mass transfer correlation proposed in the work [2]

$$Nu = 2 + 1.1 Pr^{1/3} Re^{0.6} \quad (6)$$

At lower Reynolds numbers the data are slightly higher than the solid line. In fact, Satterfield and Resnick [25] have found $J_H/J_D = 1.37$, and De Acetis and Thodos [19] $J_H/J_D = 1.51$. McConnachie and Thodos [21], Sen Gupta and Thodos [22, 23], and Mallin and Thodos [20], however, have found $J_H/J_D = 1.0$. In general, heat transfer measurements and determination of heat transfer coefficients are more difficult than mass transfer studies. Considering this, we may say that the heat transfer data shown in Fig. 2 are well represented by eqn (6).

Measurement of temperature in bed of no heat generating particles

Kunii and Smith [27], and Cybulski *et al* [28], respectively, determined the heat transfer coefficients on the Continuous Solid Phase (C-S) model from the axial and radial heat transfer measurements.

Assuming that the gas temperatures computed on the C-S model are equal to the measured temperature profiles, Cybulski *et al* obtain the coefficients. Wakao *et al* [13], however, point out that the C-S model can not be extended to the determination of heat transfer coefficients at steady state.

In fact, under steady condition, the gas temperatures calculated with low heat transfer coefficients on the C-S model agree with the temperatures computed on a single-phase model (in which heat transfer coefficient is not

involved, the temperature is considered to be almost equal to the measured temperature), but the solid temperatures evaluated on the C-S model are far different from the temperatures on the single-phase model. It is considered that if Cybulski *et al* had noticed the large difference in calculated temperature between the gas and solid, they have hesitated to determine the heat transfer coefficients.

Kunii and Smith also employ the C-S model. In addition, they determine the anomalously low heat transfer coefficients by incorrect interpretation of the algebraic relationship between the heat transfer coefficient and the effective thermal conductivity of the bed. This has been criticized by Littman *et al* [29], and Gunn and De Souza [4]. Gunn and De Souza point out that if Kunii *et al* had interpreted the algebraic relationship correctly, infinitely large heat transfer coefficients would have been obtained.

As far as no heat source or sink exists in solid particles, fluid- and solid-phase temperatures under steady state condition are considered to be substantially the same. Heat transfer coefficients cannot, therefore, be determined from the steady heat transfer measurements unless heat is generated or removed in solid particles.

Heat transfer between heat generating particles and fluid

Eichhorn and White [30], Baumeister and Bennett [31] and Pei *et al* [32, 33] have employed high-frequency heating to generate heat in solid particles.

Eichhorn and White find that the solid temperature profiles are linear function of axial distance (see their Fig. 3). The solid temperature at bed exit is then estimated by the straight line-extrapolation of the solid temperatures to the exit. They assume that the temperature difference between the solid and gas throughout the bed is the same as the difference between the solid temperature extrapolated to the bed exit and the

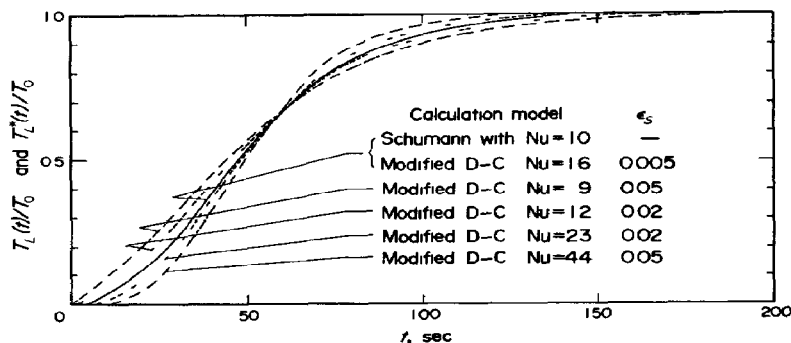


Fig. 3 Comparison of step response curves, lead-air system, $Re = 100$, $\epsilon_b = 0.36$, $D_p = 0.3$ cm, $L = 3.3$ cm, $\alpha_{ax}^* = 31$ cm²/sec

temperature of the gas leaving the bed. However, the temperature difference is small (0.9–3.8°F) and yet the solid temperature profiles seem to have relatively large errors (about 1°F in their Fig. 3) compared to the temperature difference. The obtained heat transfer coefficients are, therefore, considered to be less reliable.

Another reason for discarding their data is that the solid temperatures may not be extrapolated to the bed exit. Equations (B1–3) solved with the Danckwerts' boundary conditions show that both the solid and gas temperatures should level off at the exit. If this is the case, the temperature difference evaluated by Eichhorn *et al.* is larger than the real temperature difference in the bed.

Note that the solid temperatures in the bed being linear function of axial distance may give an impression that the axial fluid dispersion coefficient is small. However, the substitution of α_{ax}^* of eqn (5) into eqn (B3), in fact, gives almost linear increase of solid temperature in the axial direction except in the vicinity of the bed exit.

The data of Baumeister *et al.* have been criticized by Jeffreson[34] because large temperature differences existed in radial direction of the bed. Pei *et al.* found the particle temperatures uniform throughout the beds and have calculated the heat transfer coefficients under the condition of uniform particle temperature. However, there may be a question whether a uniform temperature is attained by the uniform heat generation in particles. In fact, as mentioned above, Eichhorn *et al.* found solid temperature increase in the axial direction of the bed. Baumeister *et al.* have also observed considerable difference in solid temperature between the bed inlet and outlet.

Glaser and Thodos[35] heated the particles by passing electric current directly through the bed of metal spheres. We are afraid, however, that heat must have been generated at the points of particle contact and most of the heat transfer would have taken place near the contact points.

We, therefore, conclude that all of the data reviewed in this section should not be included in the data correlation.

REVIEW AND CORRECTION OF THE DATA OBTAINED FROM NONSTEADY MEASUREMENTS

From step, frequency and shot response measurements, the heat transfer coefficients have been obtained

on any of the heat transfer models shown in Table 2: Schumann model, Continuous Solid Phase (C-S) model, and Dispersion Concentric (D-C) model.

The Schumann model[36] incorporates the following assumptions:

- (i) Fluid is in plug flow with no dispersion
- (ii) No temperature gradient in particle

The C-S model[29], when applied for axial heat transfer, has the assumptions:

- (i) Fluid is in dispersed plug flow
- (ii) Solid is in axially continuous phase through which heat conduction takes place in the axial direction

The original D-C model and the modified D-C model[12, 14], both, have the assumptions:

- (i) Fluid is in dispersed plug flow
- (ii) Concentric temperature profile in particle

The difference between the two models is that the axial fluid dispersion coefficient, α_{ax} of eqn (3), is used for the original D-C model, while the large axial effective dispersion coefficient, α_{ax}^* of eqn (4), is employed for the modified D-C model.

Gunn and De Souza[4] were the first to find, from the frequency response measurements, that the axial fluid thermal dispersion coefficients on the D-C model were considerably larger than those for extraparticle mass dispersion. Vortmeyer[37] has discussed the meaning of the large dispersion coefficient values. Wakao *et al.*[38] have also obtained, from the shot response measurements, the large thermal dispersion coefficients.

The C-S model has been criticized by Kaguel *et al.*[12], and the original D-C model by Wakao *et al.*[1, 14]. They have shown that the modified D-C model has advantage over the C-S and original D-C models. One of the important things pointed out by them is that the heat transfer coefficients determined on the C-S or original D-C model are different from those on the modified D-C model, particularly in the range of low Reynolds number.

The published nonsteady heat transfer data are, therefore, converted into those on the modified D-C model and compared with the steady heat transfer data recalculated in the preceding section. Note that the steady data have been reevaluated on the modified D-C model.

Turner *et al.*[39, 40] and Gunn and De Souza[4] have obtained, from the frequency response measurements, the heat transfer coefficients and the large axial dispersion coefficients on the D-C model. Their measure-

Table I Heat transfer work

Year	Reference No	Investigator	Experimental method	Steady or nonsteady	Particle			Fluid	Pr	Re	In determination of heat transfer coefficients		Remarks
					Material	Shape	Size, mm				Particle temperature	Fluid dispersion considered	
1943	[15]	Ganson, Thodos and Houghen	Evaporation of water	Steady	Celite	Sphere	2.3, 3.0, 5.6, 8.4, 11.6	Air	0.72-0.75	$\frac{D_p}{\mu} = 100-4,000$	Surface at wet-bulb temperature assumed	No	
1943	[17]	Hurt	Ibid	Steady		Cylinder	4.1x4.8, 6.8x8.5, 9.8x11.7, 14.0x12.5, 18.8x16.9	Air	0.76	$\frac{D_p}{\mu} = 72-950$	Measured	No	
1945	[16]	Wilke and Houghen	Ibid	Steady	Celite	Cylinder	3.1x3.1, 4.8x4.3, 6.6x7.2, 9.7x8.6, 13.4x12.8, 15.1x16.3, 18.2x16.9	Air	0.73	$\frac{D_p}{\mu} = 45-250$	Surface at wet-bulb temperature assumed	No	Heat transfer coefficients were not determined, but obtainable from their data
1952	[30]	Eichhorn and White	High frequency dielectric heating particles	Steady	Dowex-50	Sphere	0.1, 0.3, 0.4, 0.5, 0.7	Air CO ₂	0.7 0.8	$\frac{D_p}{\mu} = 1-18$	Measured	No	The measurements were criticized by Littman et al [29]
1954	[28]	Satterfield and Resnick	Decomposition of H ₂ O ₂	Steady	Polished catalytic metal	Sphere	5.1	Vapor mixture of H ₂ O & H ₂ O	1.0	$\frac{D_p}{\mu} = 15-160$	Measured	No	
1957	[18]	Galloway, Konamicky and Epstein	Evaporation of water	Steady	Celite	Sphere	17.1	Air	0.72	$\frac{D_p}{\mu} = 150-1,200$	Measured	No	
1958	[35]	Glaser and Thodos	Heating metallic particles by passing electric current through beds	Steady	None	Sphere	4.8	Air	0.71	$\frac{\sqrt{A_p G}}{\mu(1-\epsilon_b)\psi} = 100-9,200$	Measured	No	
					Brass	Sphere	5.4, 7.9	H ₂ CO ₂	0.72 0.67	A _p particle surface area ψ shape factor			
					Steel	Cylinder	5.4, 9.5						
						Cube	6.4, 9.5						
1958	[34]	Baumeister and Bennett	High frequency induction heating particles	Steady	Steel	Sphere	3.9, 6.3, 9.5	Air	0.7	$\frac{D_p}{\mu} = 200-10,400$	Measured	No	The measurements were criticized by Jeffreson[34]
1960	[19]	De Acetis and Thodos	Evaporation of water	Steady	Celite	Sphere	15.9	Air	0.72	$\frac{D_p}{\mu} = 32-2,100$	Measured	No	
1961	[27]	Kunii and Smith	Axial heat conduction in beds	Steady	Glass Sand	Sphere	0.1, 0.4, 0.6, 1.0 0.1, 0.2	He, Air, CO ₂ , Water		$\frac{D_p}{\mu} = 0.001-1$	Continuous solid phase with axial heat conduction assumed	Yes	The anomalously low Nu data were criticized by Littman et al [29] and Gunn et al [4]
1963	[21]	McComachie and Thodos	Evaporation of water	Steady	Celite	Sphere	15.9	Air	0.72	$\frac{D_p}{u(1-\epsilon_b)} = 110-2,500$	Measured	No	

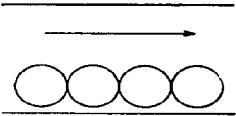
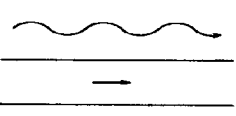
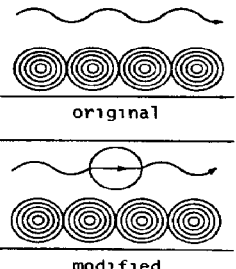
Table 1 (Contd)

Year Reference No	Investigator	Experimental method	Steady or nonsteady	Particle			Fluid	Pr	Re	In determination of heat transfer coefficients		Remarks
				Material	Shape	Size, mm				Particle temperature	Fluid dispersion considered	
1963 [24]	Bradshaw and Myers	Evaporation of water	Steady	Kaoline AMT	Sphere	4.7 8.8	Air	0.7	$\frac{D.G}{\mu(1-\epsilon_p)} = 400-6,500$	Measured	No	
				Kaolorb	Cylinder	4.0x4.1						
				Celite	Cylinder	4.2x4.2, 6.2x4.9						
1963 [22]	San Gupta and Thodos	Ibid	Steady	Celite	Sphere	15.9	Air	0.72	$\frac{D.G}{\mu} = 800-2,000$	Measured	No	
1964 [23]	San Gupta and Thodos	Ibid	Steady	Celite	Sphere	15.9	Air	0.72	$\frac{D.G}{\mu} = 2,000-6,000$	Measured	No	
1967 [20]	Malling and Thodos	Ibid	Steady	Celite	Sphere	15.7-15.9	Air	0.71	$\frac{D.G}{\mu} = 185-8,500$	Measured	No	
1967 [47]	Lindauer	Frequency response	Nonsteady	Steel Tungsten	Sphere	1.0, 1.8, 3.2 0.5	Air	0.7	$\frac{D.G}{\mu} = 23-18,200$	No temperature gradient in particle assumed	No	
1968 [45]	Handley and Heggis	Step response	Nonsteady	Steel	Sphere	3.2, 6.4, 9.5	Air	0.7	$\frac{D.G}{\mu} = 80-4,000$	No temperature gradient in particle assumed	No	The data were corrected by Jefferson [34] for fluid dispersion
				Lead	Sphere	3.0, 6.1, 9.1						
				Bronze	Sphere	9.5						
				Soda glass	Sphere	6.1, 9.1						
				Lead glass	Sphere	3.0						
				Alumina-silica	Sphere	3.2						
1968 [29]	Littman, Barile and Pulsifer	Frequency response	Nonsteady	Copper Glass Lead	Sphere	0.5, 0.6, 0.7, 1.1 0.5 2.0	Air	0.7	$\frac{D.G}{\mu} = 2-100$	Continuous solid phase with axial heat conduction assumed	Yes	The method of determining μ data was criticized by Kaguei et al [12]
1970 [46]	Bradshaw, Johnson, McLachlan and Chiu	Step response	Nonsteady	Alumina Steel Hematite	Sphere	13.2, 25.4 25.2 11.1	Air, N ₂	0.74	$\frac{D.G}{6\mu(1-\epsilon_p)} = 150-600$	Center-symmetric temperature profile in particle assumed	Yes	
1971 [39]	Goss and Turner	Frequency response	Nonsteady	Soda lime glass Borosilicate glass Methyl methacrylate	Sphere	4.0 5.0 4.8	Air	0.7	$\frac{D.G}{\mu} = 1,600-3,000$	Center-symmetric temperature profile in particle assumed	Yes	

1973	[40]	Turner and Otten	Frequency response	Nonsteady	Soda lime glass	Sphere	4 0	Air	0.7	$\frac{D_p G}{\mu} = 1,200-4,600$	Center-symmetric temperature profile in particle assumed	Yes
					Ceramic	Spheroid	7.4					
					Sintered glass		4.6					
					Fertilizer		3.1					
					Iron ore		4.8					
					Epoxy	Sphere	3.5					
1974	[32]	Balakrishnan and Pei	Microwave heating particles	Steady	Iron oxide	Sphere	6.4	Air	0.7	$\frac{D_p G}{\mu(1-\epsilon_p)} = 340-4,400$	Measured	No
					Nickel oxide	Sphere	6.4, 12.7					
					Vanadium pentoxide	Sphere	4.8					
						Cylinder	5.6x5.6, 5.6x8.3					
					Nickel-molybdenum oxide	Cylinder	3.2x6.4					
					Cobalt-molybdenum	Cylinder	3.2x6.4					
1974	[4]	Gunn and De Souza	Frequency response	Nonsteady	Glass	Sphere	0.3, 0.5, 1.2, 2.2, 3.0, 6.0	Air	0.7	$\frac{D_p G}{\mu} = 0.05-330$	Center-symmetric temperature profile in particle assumed	Yes
					Steel	Sphere	3.2, 6.3					
					Lead	Sphere	0.8					
1975	[33]	Bhattacharyya and Pei	Microwave heating particles	Steady	Ferric oxide	Sphere	3.2, 7.6	Air	0.7	$\frac{D_p G}{\mu} = 110-830$	Measured	No
						Cylinder	5.1x5.1					
1975	[28]	Cybulski, Van Dalen, Verkerk and Van Den Berg	Radial heat conduction in beds	Steady	Silicon-copper	Irregular	0.1	Air	0.7	$\frac{D_p G}{\mu} = 0.24-0.64$	Continuous solid phase with radial heat conduction assumed	No
												The anomalously low Nu data were criticized by Makao et al [13]
1976	[38]	Makao, Tanisho and Shirozawa	Shot response	Nonsteady	Polystyrene	Sphere	0.8	Air	0.7	$\frac{D_p G}{\mu} = 0.2-6$	Center-symmetric temperature profile in particle assumed	Yes
					Glass	Sphere	0.3, 1.1, 1.6					No definite Nu data were obtained, but it was shown that Nu cannot be smaller than 0.1
					Lead	Sphere	0.9					

Diluted beds, distended beds and data with single particle layer are not included

Table 2 Heat transfer models and fundamental equations

Model	Assumptions	Fundamental equations
Schumann model 	Fluid in plug flow No temperature gradient within particle	$\frac{\partial T_F}{\partial t} = -u \frac{\partial T_F}{\partial x} - \frac{h_p a}{\epsilon_b C_F \rho_F} (T_F - T_S),$ $(1 - \epsilon_b) \frac{\partial T_S}{\partial t} = \frac{h_p a}{C_S \rho_S} (T_F - T_S)$
Continuous Solid Phase (C-S) model 	Fluid in dispersed plug flow Axial heat conduction in solid phase	$\frac{\partial T_F}{\partial t} = \frac{k_{ef}}{\epsilon_b C_F \rho_F} \frac{\partial^2 T_F}{\partial x^2} - u \frac{\partial T_F}{\partial x} - \frac{h_p a}{\epsilon_b C_F \rho_F} (T_F - T_S),$ $(1 - \epsilon_b) \frac{\partial T_S}{\partial t} = \frac{k_{es}}{C_S \rho_S} \frac{\partial^2 T_S}{\partial x^2} + \frac{h_p a}{C_S \rho_S} (T_F - T_S)$
Dispersion Concentric (D-C) model 	Fluid in dispersed plug flow Dispersion coefficient of Eqn(3) for original D-C model, that of Eqn(4) for modified D-C model Particle temperature with radial symmetry	$\frac{\partial T_F}{\partial t} = \alpha_{ax} \frac{\partial^2 T_F}{\partial x^2} - u \frac{\partial T_F}{\partial x} - \frac{h_p a}{\epsilon_b C_F \rho_F} (T_F - (T_S)_R),$ $\frac{\partial T_S}{\partial t} = \alpha_S \left(\frac{\partial^2 T_S}{\partial r^2} + \frac{2}{r} \frac{\partial T_S}{\partial r} \right),$ $\text{at } r = R, \quad k_S \left(\frac{\partial T_S}{\partial r} \right) = h_p (T_F - T_S)$

ments obviously support the modified D-C model, but their data are examined in sensitivity

Step response

Step response measurements were made by Furnas[41], Saunders and Ford[42], Lof and Hawley[43], Coppage and London[44], Handley and Heggs[45], and Bradshaw *et al* [46]. Except Bradshaw *et al* who employed the D-C model, all of them have determined the heat transfer coefficients on the Schumann model. However, in the early studies[41–44] the heat transfer coefficients seem to have been determined by less reliable graphical method.

The data of the two relatively recent measurements, Handley *et al* [45] and Bradshaw *et al* [46], are reevaluated on the modified D-C model. Handley *et al* have obtained the heat transfer coefficients on the Schumann model. The exact solution to a step response is shown in Appendix D. Using the Schumann model solution, the response curves $T_L(t)$ of Handley *et al* are predicted with the data reported in their paper. The response curves $T_F(t)$ are also calculated on the modified D-C model with varied heat transfer coefficient values. Figure 3 illustrates the comparison of $T_L(t)$ and $T_F(t)$. The error ϵ_s is calculated by

$$\epsilon_s = \sqrt{\left(\frac{1}{\tau_2 - \tau_1} \int_{\tau_1}^{\tau_2} \left[\frac{T_L(t) - T_F(t)}{T_0} \right]^2 dt \right)} \quad (7)$$

where we choose the times, τ_1 and τ_2 , respectively, as $T_L(\tau_1) = 0.05T_0$ and $T_L(\tau_2) = 0.95T_0$.

We may probably say that the agreement of the two curves is good when $\epsilon_s < 0.02$. In Fig. 4 some of the original data of Handley *et al* are compared with those

reevaluated on the modified D-C model. Some of the recalculated data are plotted with the range indicating $\epsilon_s < 0.02$. It is seen that the data reevaluated on the modified D-C model become considerably higher, as Reynolds number decreases, than the original data on the Schumann model.

The data of Bradshaw *et al* obtained on the D-C model are also reevaluated. In the recalculation on the modified D-C model we assume that a step temperature change is imposed on the inlet fluid. As shown in Fig. 5, their original heat transfer coefficients obtained on the D-C model are in good agreement with the reevaluated data on the modified D-C model. Some of the reevaluated data are again plotted with the range indicating

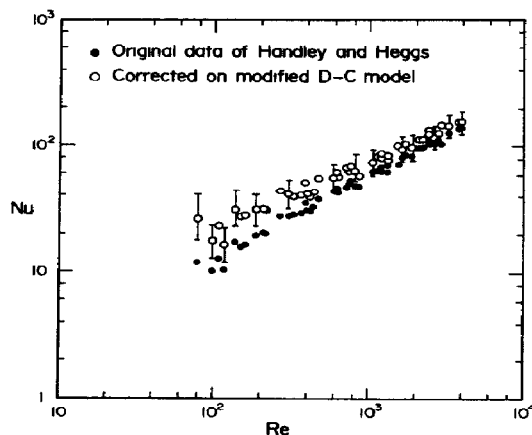


Fig. 4 Data obtained by Handley and Heggs[45] and those reevaluated on modified D-C model. The range indicates $\epsilon_s < 0.02$

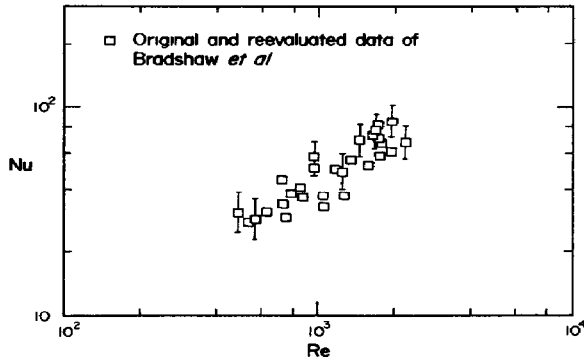


Fig 5 Original data obtained by Bradshaw *et al* [46] and those reevaluated on modified D-C model. The original and reevaluated data are in good agreement. The range indicates $\epsilon_s < 0.02$

$\epsilon_s < 0.02$ The reason for the agreement is that the measurements were made at high Reynolds numbers ($Re = 490-2200$) so that the axial fluid dispersion coefficients they assumed are close to the α_{ax}^* values

Frequency response

The heat transfer coefficients have been obtained from frequency response measurements by Lindauer [47], Littman *et al* [29], Littman and Shiva [3], Goss and Turner [39], Turner and Otten [40], and Gunn and De Souza [4]

Lindauer employed the same fundamental equations used for the Schumann model, but no information on the frequency range has been given in his paper. The heat transfer data cannot, therefore, be converted into those on the modified D-C model

Littman *et al* also employed the C-S model. Kaguei *et al* [12] examined the heat transfer data on the C-S model and have found that the heat transfer coefficients on the model decrease anomalously with decrease of flow rates, but the coefficients determined on the modified D-C model never decrease

Turner *et al* [39, 40] and Gunn and De Souza [4] have obtained not only the heat transfer coefficients but also the axial thermal dispersion coefficients on the D-C model

With the data of Gunn and De Souza reported in their paper [4], their frequency response curves $T_L(t)$ are predicted. The curves $T_L^+(t)$ on the D-C model are also calculated as a function of α_{ax} and Nu. Note that $T_L(t)$ and $T_L^+(t)$ are calculated from eqn (C7) in Appendix C

A comparison of $T_L(t)$ and $T_L^+(t)$ is illustrated with the error figures in Fig 6. The error is the difference between the solid curve $T_L(t)$ and the other curves $T_L^+(t)$

$$\epsilon_f = \sqrt{\frac{\int_0^{2\pi/\omega} [T_L(t) - T_L^+(t)]^2 dt}{\int_0^{2\pi/\omega} [T_L(t)]^2 dt}} \quad (8)$$

We may again say that the two curves are in good agreement if the error is less than 5%

Figures 7(a) and (b) show error maps. The valley with

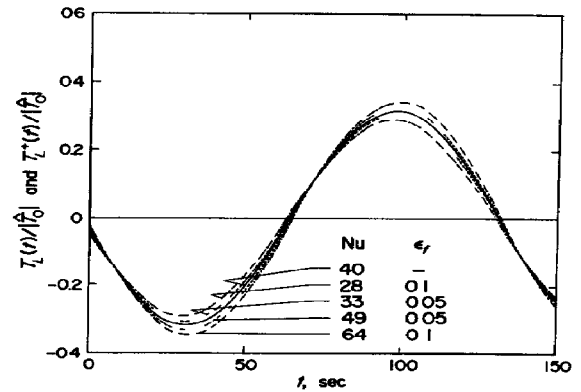


Fig 6 Comparison of frequency response curves calculated on D-C model, glass-air system, $Re \approx 33$, $\epsilon_b = 0.4$, $D_p = 0.22$ cm, $L = 3.0$ cm, $\omega = 0.015\pi$ rad/sec, $\alpha_{ax} = 7.3$ cm²/sec

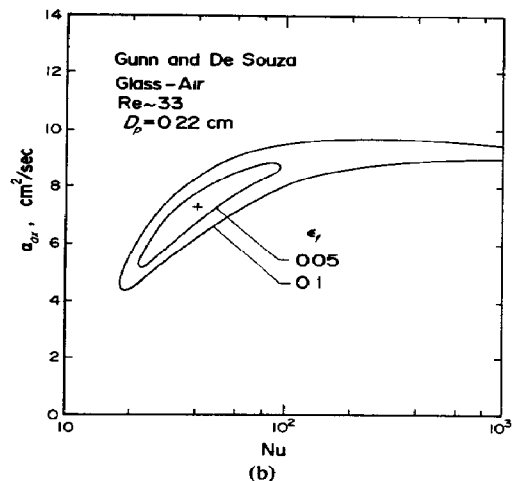
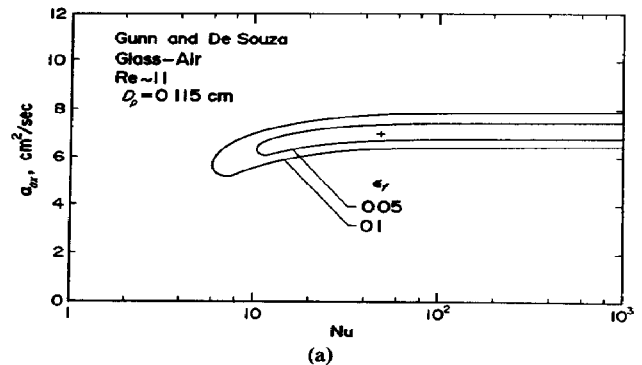


Fig 7 Error map for data of Gunn and De Souza [4] (+ shows the data obtained by them), (a) $Re = 11$, $\epsilon_b = 0.4$, $D_p = 0.115$ cm, $L = 3.0$ cm, amplitude ratio = 0.3, α_{ax}^* of eqn (5) = 5.6 cm²/sec (b) $Re \approx 33$, $\epsilon_b = 0.4$, $D_p = 0.22$ cm, $L = 3.0$ cm, amplitude ratio = 0.3, α_{ax}^* of eqn (5) = 10 cm²/sec

small error (say, $\epsilon_f = 0.05$) indicates that Nusselt numbers cannot be determined at low flow rates, although Gunn *et al* have determined the definite values of α_{ax} and Nu. According to the valley with $\epsilon_f = 0.05$, Nusselt numbers are determined in range, i.e. $Nu > 10$ from Fig 7(a), and $Nu = 20-90$ from Fig 7(b). The

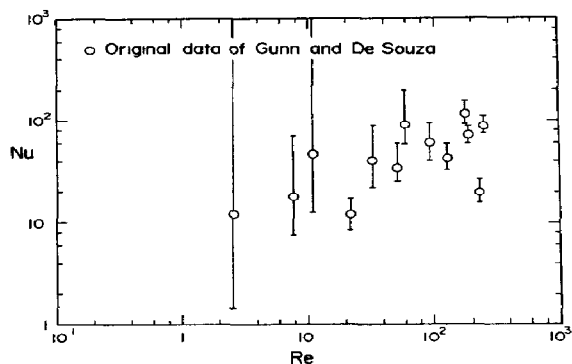


Fig 8 Range of Nusselt numbers with $\epsilon_f < 0.05$, for Gunn and De Souza[4]

obtained Nusselt number ranges are shown in Fig 8. The ranges are very large at low Reynolds numbers, and yet their original data scatter considerably. We do not, therefore, use the data of Gunn and De Souza in our data correlation.

No detailed information on frequency values employed in the experiments is given in the papers of Goss and Turner[39], and Turner and Otten[40] so that their data cannot be examined. There is, however, an example presented for simulation calculation in the paper of Goss and Turner (their Table 1 in Part II). The example ($Re = 950$) is, therefore, examined in sensitivity (by using eqns (C5) and (C6)). As shown in Fig 9, the valley with the error 0.05 is steep. As far as the example is concerned, the determined Nusselt number is considered to be enough reliable.

In fact, the experiments of Turner *et al* were conducted at high Reynolds numbers 1200–4600. As mentioned already, reliable heat transfer coefficients are determined at high flow rates. The data of Turner *et al* are, therefore, included in our data correlation.

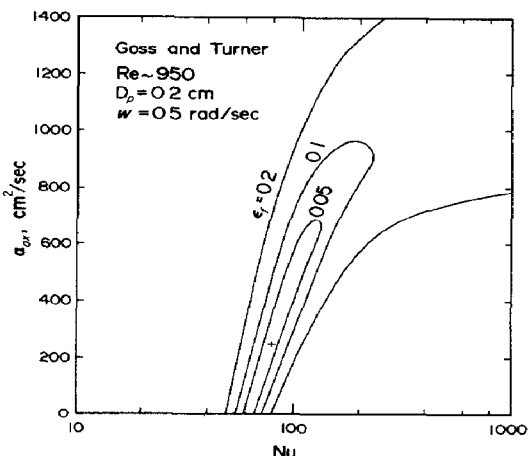


Fig 9 Error map for a simulation illustration of Goss and Turner[39] (+ shows the data obtained by them), $Re = 950$, $\omega = 0.5$ rad/sec, other data shown in their Table 1, $\alpha_{w, \text{eqn (5)}} = 250 \text{ cm}^2/\text{sec}$

Shot response

From the analysis of shot response measurements, Wakao *et al* [1, 38] examined the heat transfer coefficients on the modified D-C model, pointing out the advantage of the model. No definite Nusselt numbers were obtained, but they have found that Nusselt numbers were considered to be in the range from 0.1 to ∞ at Reynolds numbers 0.2–6.

CORRELATION OF NUSSELT NUMBERS

From the review in the preceding sections the heat transfer data which have passed our criteria are [16, 18–23, 25, 39, 40, 45, 46]. Their heat transfer coefficients reevaluated on the modified D-C model are plotted in Fig 10. The data are well represented by the analogous expression of mass correlation, eqn (6).

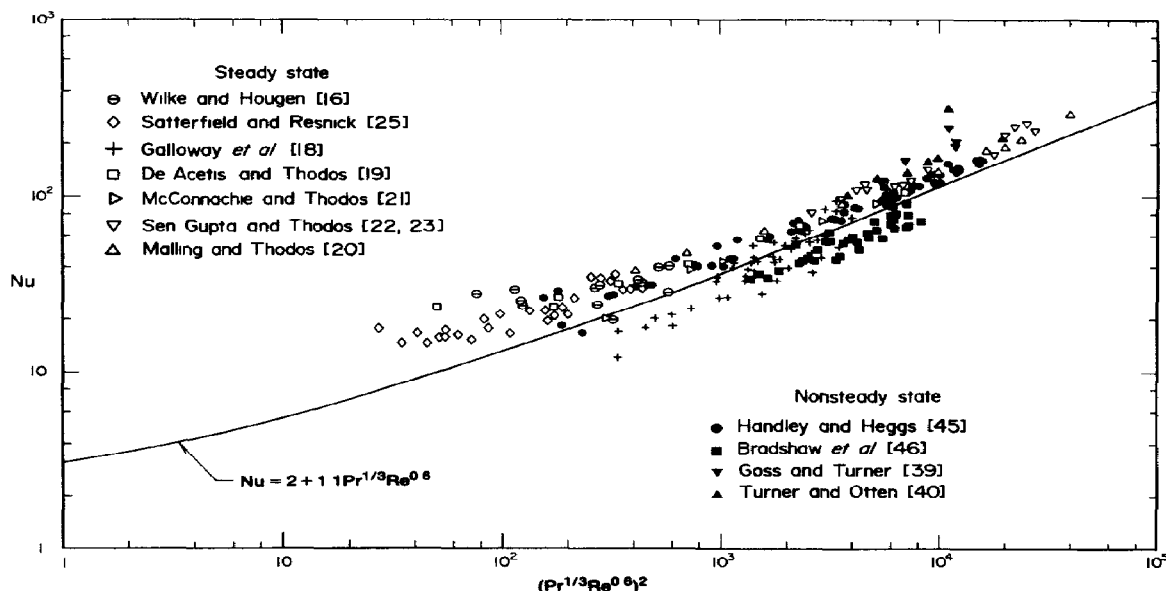


Fig 10 Correlation of reevaluated Nusselt numbers

One more thing we have to pay attention to is that Fig 1 shows the mixture of heat transfer data obtained on the different models. Some of them are, as mentioned already, less reliable and some have been criticized on the calculation procedure.

CONCLUSIONS

1 The published heat transfer data are corrected for the axial fluid thermal dispersion coefficients proposed by Wakao [1]. The reevaluated data on the modified D-C model are correlated by the analogous form of the mass transfer correlation, eqn (6).

2 When the heat transfer correlation is used for the design and analysis of packed bed reactors, the axial effective thermal dispersion coefficients given by eqn (4) should also be employed.

NOTATION

a	particle surface area per unit volume of packed bed
C_F	specific heat of fluid
C_S	specific heat of solid
D_p	particle diameter
G	$\epsilon_b U \rho_F$, fluid mass velocity
h_p	heat transfer coefficient
h'_p	heat transfer coefficient determined with $\alpha_{ax} = 0$
J_D, J_H	J -factors, respectively, for mass and heat
k_e^0	effective thermal conductivity of packed bed with stagnant fluid
$k_{e,ax}$	axial effective thermal conductivity of packed bed
k_{ef}	effective fluid thermal conductivity
k_{es}	effective solid thermal conductivity
k_F	fluid thermal conductivity
k_S	solid thermal conductivity
L	packed bed height
Nu	$h_p D_p / k_F$, Nusselt number
Pr	$C_F \mu / k_F$, Prandtl number
R	particle radius
r	radial distance variable
Re	$D_p \epsilon_b U \rho_F / \mu$, Reynolds number
T_F	fluid temperature
T_{in}	inlet fluid temperature
T_L	fluid temperature at bed exit
T_L^*	fluid temperature at bed exit calculated on modified D-C model
T_L^+	fluid temperature at bed exit calculated on D-C model with varied α_{ax} and Nu
T_0	temperature change imposed on inlet fluid
T_{ps}	temperature on particle surface
T_S	solid temperature
\hat{T}	amplitude in complex
t	time
U	interstitial fluid velocity
x	axial distance variable

Greek symbols

α_{ax}	axial fluid thermal dispersion coefficient
α_{ax}^*	axial effective thermal dispersion coefficient, defined by eqn (4)
α_F	fluid thermal diffusivity

α_S	solid thermal diffusivity
ϵ_b	bed void fraction
ϵ_f	error defined by eqn (8)
ϵ_s	error defined by eqn (7)
ρ_F	fluid density
ρ_S	solid density
τ_1, τ_2	times
μ	fluid viscosity
ω	frequency

REFERENCES

- [1] Wakao N, *Chem Engng Sci* 1976 **31** 1115
- [2] Wakao N and Funazkri T, *Chem Engng Sci* 1978 **33** 1375
- [3] Littman H and Silva D E, *Proc Int'l Heat Transfer Conf Versailles*, Paper CT1.4 (1970)
- [4] Gunn D J and De Souza J F C, *Chem Engng Sci* 1974 **29** 1363
- [5] Cornish A R H, *Trans Instn Chem Engrs* 1965 **43** T332
- [6] Kunii D and Suzuki M, *Int J Heat Mass Trans* 1967 **10** 845
- [7] Nelson P A and Galloway T R, *Chem Engng Sci* 1975 **30** 1
- [8] Schlünder E U, *Chem Engng Sci* 1977 **32** 845
- [9] Pfeffer R and Happel J, *A I Ch E J* 1964 **10** 605
- [10] Miyauchi T, *J Chem Engng Japan* 1971 **4** 238
- [11] Sørensen J P and Stewart W E, *Chem Engng Sci* 1974 **29** 827
- [12] Kaguei S, Shiozawa B and Wakao N, *Chem Engng Sci* 1977 **32** 507
- [13] Wakao N, Kaguei S and Nagai H, *Chem Engng Sci* 1977 **32** 1261
- [14] Wakao N, Kaguei S and Shiozawa B, *Chem Engng Sci* 1977 **32** 451
- [15] Gamson B W, Thodos G and Hougen O A, *Trans Am Inst Chem Engrs* 1943 **39** 1
- [16] Wilke C R and Hougen O A, *Trans Am Inst Chem Engrs* 1945 **41** 445
- [17] Hurt D M, *Ind Engng Chem* 1943 **35** 522
- [18] Galloway L R, Komarnicky W and Epstein N, *Can J Chem Engng* 1957 **35** 139
- [19] De Acetis J and Thodos G, *Ind Engng Chem* 1960 **52** 1003
- [20] Mallin G F and Thodos G, *Int J Heat Mass Trans* 1967 **10** 489
- [21] McConachie J T L and Thodos G, *A I Ch E J* 1963 **9** 60
- [22] Sen Gupta A and Thodos G, *A I Ch E J* 1963 **9** 751
- [23] Sen Gupta A and Thodos G, *Ind Engng Chem Fundls* 1964 **3** 218
- [24] Bradshaw R D and Myers J E, *A I Ch E J* 1963 **9** 590
- [25] Satterfield C N and Resnick H, *Chem Engng Progr* 1954 **50** 504
- [26] Wakao N and Kato K, *J Chem Engng Japan* 1969 **2** 24
- [27] Kunii D and Smith J M, *A I Ch E J* 1961 **7** 29
- [28] Cybulski A, Van Dalen M J, Verkerk J W and Van Den Berg P J, *Chem Engng Sci* 1975 **30** 1015
- [29] Littman H, Barile R G and Pulsifer A H, *Ind Engng Chem Fundls* 1968 **7** 554
- [30] Eichhorn J and White R R, *Chem Engng Progr Symp Ser* 1952 **48** (4) 11
- [31] Baumeister E B and Bennett C O, *A I Ch E J* 1958 **4** 69
- [32] Balakrishnan A R and Pei D C T, *Ind Engng Chem Proc Des Dev* 1974 **13** 441
- [33] Bhattacharyya D and Pei D C T, *Chem Engng Sci* 1975 **30** 293
- [34] Jeffreson C P, *A I Ch E J* 1972 **18** 409
- [35] Glaser M B and Thodos G, *A I Ch E J* 1958 **4** 63
- [36] Schumann T E W, *J Franklin Inst* 1929 **208** 405
- [37] Vortmeyer D, *Chem Engng Sci* 1975 **30** 999
- [38] Wakao N, Tanisho S and Shiozawa B, *Kagaku Kogaku Ronbunshu (Japan)* 1976 **2** 422
- [39] Goss M J and Turner G A, *A I Ch E J* 1971 **17** 590
- [40] Turner G A and Otten L, *Ind Engng Chem Proc Des Dev* 1973 **12** 417

- [41] Furnas C C, *Ind Engng Chem* 1930 22 721
 [42] Saunders O A and Ford H, *J Iron Steel Inst* 1940 141 291
 [43] Lof G O G and Hawley R W, *Ind Engng Chem* 1948 40 1061
 [44] Coppage J E and London A L, *Chem Engng Progr* 1956 52 57-F
 [45] Handley D and Heggs P J, *Trans Instn Chem Engrs* 1968 46 T251
 [46] Bradshaw A V, Johnson A, McLachlan N H and Chiu Y-T, *Trans Instn Chem Engrs* 1970 48 T77
 [47] Lindauer G C, *AIChE J* 1967 13 1181

APPENDIX A STEADY HEAT TRANSFER BETWEEN FLUID AND PARTICLE SURFACE AT CONSTANT TEMPERATURE

For heat transfer between fluid and particles having constant surface temperature T_{ps} throughout the bed of finite length, the change in fluid temperature is given by (refer to eqn (7) in [2])

$$\frac{T_{ps} - T_L}{T_{ps} - T_{in}} = \frac{4A \exp\left[\frac{UL}{2\alpha_{ax}^*}\right]}{(1+A)^2 \exp\left[A \frac{UL}{2\alpha_{ax}^*}\right] - (1-A)^2 \exp\left[-A \frac{UL}{2\alpha_{ax}^*}\right]} \quad (A1)$$

where

$$A = \sqrt{\left(1 + \frac{4ah_p\alpha_{ax}^*}{\epsilon_b U^2 C_{FPF}}\right)}$$

When $\alpha_{ax}^* = 0$ eqn (A1) reduces to

$$\frac{T_{ps} - T_L}{T_{ps} - T_{in}} = \exp\left[-\frac{h_p' a L}{\epsilon_b U C_{FPF}}\right] \quad (A2)$$

Conversion of h_p' into h_p is, therefore made by equating eqns (A1) and (A2)

APPENDIX B STEADY HEAT TRANSFER FROM HEAT GENERATING PARTICLES

When heat is generated at constant rate in particles the fluid and solid temperatures in the bed of finite length are

$$T_F = T_{in} + \frac{L}{U} \left(\frac{q}{C_{FPF}} \right) \left(\frac{1 - \epsilon_b}{\epsilon_b} \right) \times \left[\frac{x}{L} + \frac{\alpha_{ax}}{UL} \left\{ 1 - \exp\left[-\frac{UL}{\alpha_{ax}} \left(1 - \frac{x}{L}\right)\right] \right\} \right] \quad (B1)$$

and

$$T_S = T_F + \frac{qR}{3h_p} + \frac{q}{6k_S} (R^2 - r^2) \quad (B2)$$

where q = heat generation rate per unit volume of particle. The solid temperatures Eichhorn and White[30] claim to have measured are the particle-volume-mean-temperatures \bar{T}_S

$$\bar{T}_S = T_F + \frac{qR}{3h_p} \left(1 + \frac{Rh_p}{5k_S} \right) \quad (B3)$$

APPENDIX C FREQUENCY RESPONSE

For the fundamental equations listed in Table 2, the boundary condition on the Schumann model is

$$\text{at } x = 0 \quad T_F = \text{Re} [\hat{T}_0 e^{i\omega t}] \quad (C1)$$

and those on D-C model are

$$\left. \begin{array}{l} \text{at } x = 0, \quad U(T_F - \text{Re} [\hat{T}_0 e^{i\omega t}]) = \alpha_{ax} \frac{\partial T_F}{\partial x} \\ \text{at } x = L, \quad \frac{\partial T_F}{\partial x} = 0 \end{array} \right\} \quad (C2)$$

When the stationary solution of T_F at $x = L$ is expressed as

$$T_L = \text{Re} [\hat{T}_L e^{i\omega t}] \quad (C3)$$

on Schumann model \hat{T}_L is

$$\frac{\hat{T}_L}{\hat{T}_0} = \exp\left[-\frac{sL}{U} \left(1 + \frac{k_1}{1 + k_2}\right)\right] \quad (C4)$$

where

$$k_1 = \frac{h_p a}{(1 - \epsilon_b) C_{SPS}}$$

$$k_2 = \frac{h_p a}{\epsilon_b C_{FPF}}$$

$$s = i\omega$$

and on D-C model,

$$\frac{\hat{T}_L}{\hat{T}_0} = \frac{\exp\left[\frac{UL}{2\alpha_{ax}}\right]}{\cosh\left[\frac{UL}{2\alpha_{ax}} \sqrt{(1+B)}\right] + \frac{1+(B/2)}{\sqrt{(1+B)}} \sinh\left[\frac{UL}{2\alpha_{ax}} \sqrt{(1+B)}\right]} \quad (C5)$$

where

$$B = \frac{4\alpha_{ax}s}{U^2} \left[1 + \frac{k_S a}{s R \epsilon_b C_{FPF}} \frac{1}{h_p R + \frac{1}{\phi \coth \phi - 1}} \right]$$

$$\phi = R \sqrt{(s/\alpha_S)}$$

In both Schumann and D-C model, the error ϵ_f of eqn (8) is

$$\epsilon_f = \frac{|\hat{T}_L - \hat{T}_L^*|}{|\hat{T}_L|} \quad (C6)$$

Using eqn (C1), Gunn *et al* [4] have obtained the semi-infinite solution of the fundamental equations

$$\frac{\hat{T}_L}{\hat{T}_0} = \exp\left[\frac{UL}{2\alpha_{ax}} (1 - \sqrt{(1+B)})\right] \quad (C7)$$

APPENDIX D STEP RESPONSE

The initial and boundary conditions for Schumann model are

$$\left. \begin{array}{l} \text{at } t = 0, \quad T_F = 0 \\ \text{at } x = 0, \quad T_F = T_0 \end{array} \right\} \quad (D1)$$

and those for D-C model are

$$\left. \begin{array}{l} \text{at } t = 0, \quad T_F = 0 \\ \text{at } x = 0, \quad U(T_F - T_0) = \alpha_{ax} \frac{\partial T_F}{\partial x} \\ \text{at } x = L, \quad \frac{\partial T_F}{\partial x} = 0 \end{array} \right\} \quad (D2)$$

The solution is

$$\frac{T_L}{T_0} = \frac{1}{2} + \frac{2}{\pi} \sum_{n=1}^{\infty} \frac{1}{2n-1} \text{Im} \left[\left(\frac{\hat{T}_L}{\hat{T}_0} \right) e^{i\omega_n t} \right]_{\omega=\omega_n} \quad (D3)$$

where $\omega_n = (2n-1)\pi/t_0$ and t_0 is a time sufficiently long enough to attain $T_L = T_0$. \hat{T}_L/\hat{T}_0 is given for Schumann model by eqn (C4) and for D-C model by eqn (C5)

The error of eqn (7) is approximately expressed as

$$\epsilon_s = \left[\frac{1}{\tau_2 - \tau_1} \int_0^{t_0} \left[\frac{T_L - T_L^*}{T_0} \right]^2 dt \right]^{1/2}$$

$$= \left[\frac{2}{\pi^2} \frac{t_0}{\tau_2 - \tau_1} \sum_{n=1}^{\infty} \frac{1}{(2n-1)^2} \frac{|\hat{T}_L - \hat{T}_L^*|_{\omega=\omega_n}^2}{|\hat{T}_0|^2} \right]^{1/2} \quad (D4)$$